

Conjugating MMAE to a novel anti-HER2 antibody for selective targeted delivery

L. LI^{1,2}, M.-Z. XU¹, L. WANG³, J. JIANG⁴, L.-H. DONG¹, F. CHEN²,
K. DONG², H.-F. SONG¹

¹State Key Laboratory of Proteomics, Beijing Proteome Research Center, National Center for Protein Sciences (Beijing), Beijing Institute of Lifeomics, Beijing, China

²Beijing United-Power Pharma Tech Co., Ltd., Beijing, China

³RemeGen, Ltd., Yantai, China

⁴Department of Pharmacology, Binzhou Medical University, Yantai, China

Abstract. – **OBJECTIVE:** To investigate the target delivery properties of RC48-ADC, a novel antibody drug conjugate (ADC) comprising cytotoxic monomethyl auristatin E (MMAE) and an anti-human epidermal growth factor receptor 2 (HER2) antibody tethered via valine-citrulline linker, *in vitro* and *in vivo*.

MATERIALS AND METHODS: Dissociation rate of MMAE from RC48-ADC was used as an estimate of its stability in serum. Cytotoxicity of the antibody and RC48-ADC towards multiple cell lines was measured. Subcellular distribution of the drug was determined by fluorescence imaging. The mechanism of lysosome targeting was verified. Endocytic pathways of RC48-ADC were assessed by the cellular fluorescence intensity of fluorescently-labelled drugs. Intracellular and extracellular distribution of MMAE was analysed after RC48-ADC or MMAE administration to characterize MMAE release. The serum and tumour concentration of MMAE was compared after tail-vein injection of RC48-ADC into tumour-bearing mice.

RESULTS: RC48-ADC was highly stable in human serum. HER2-overexpressed cell line SK-BR-3 proliferation was stronger when suppressed by RC48-ADC than by the naked antibody. Both RC48-ADC and naked antibody were internalized via caveolae-mediated and clathrin-mediated endocytosis and concentrated in lysosomes. Higher HER2 expression was associated with enhanced uptake and intracellular release of conjugated MMAE; free MMAE could kill tumour cells via the bystander effect. Although serum RC48-ADC concentration was higher than that in tumours, exposure of MMAE in tumours was ~200 times higher than in serum, which rationalized the reduced toxicity of RC48-ADC.

CONCLUSIONS: *In vitro* and *in vivo* experiments confirmed the targeted transport and release of RC48-ADC; it could selectively deliver MMAE to the targeted HER2-positive cell or tu-

mour tissue, which could reduce off-target toxicity and enhance anti-tumour potency in humans.

Key Words:

Antibody-drug-conjugate (ADC), Cytotoxicity, Internalization, Targeted delivery, Monomethyl auristatin E (MMAE), Human epidermal growth factor receptor (HER)2, Valine-Citrulline linker.

Introduction

Small molecule chemotherapeutic drugs form a considerable portion of front-line regimens for most tumour types, but systemic toxicity remains their primary shortcoming. Monoclonal antibody therapy has demonstrated effective anti-tumour activity, but long-term efficacy tends to be poor due to the development of drug resistance¹. Antibody-drug conjugates (ADCs), which are combinations of antibodies and highly potent cytotoxins, can improve the therapeutic index and reduce the systemic toxicity related to cytotoxic payload². Suppressing the cytotoxicity of the payload when the drug passes through blood circulation is important for ADC design, which is the motivation behind conjugating cytotoxic drug to an antibody. Selective targeted delivery and release of payloads to tumour tissue sites can reduce the off-target effects in non-expressing antigen cells. There are five FDA-approved ADCs on the market, namely ADCETRIS[®], MYLOTARG[®], BE-SPONSA[®], POLIVY[®], and KADCYLA[®]. Except for KADCYLA[®], which is for Human epidermal growth factor receptor 2 (HER2) overexpressed solid tumours, those ADCs are for hematological tumour treatment. The dose of the antibody delivered to the target site accounts for < 0.01% within 24 h af-

ter administration³. The transport and targeted payload release of ADCs at tumour sites is crucial for determining their efficacy and safety^{4,5}, as solid tumours tend to have more heterogeneous expression of targetable tumour markers. HER2 is a member of the epidermal growth factor family of receptors that is overexpressed in 12-23% of breast cancers and 18-28% of gastric cancers⁶, and is also overexpressed in a broad range of solid tumours, including esophageal, ovarian, endometrial, bladder, colorectal, and head/neck cancers⁷. MMAE is a synthetic derivative of auristatin with anti-mitotic effect⁸, which has been widely used as a cytotoxic component for the preparation of ADCs^{9,10}. The valine-citrulline (VC) linker is stable, and can only be cleaved by cathepsins when ADCs are endocytosed into lysosomes, resulting in the release of payloads to kill target cancer cells¹¹. Anti-HER2 antibody-Val-Cit-MMAE (RC48-ADC) consists of monomethyl auristatin E (MMAE) bound to a humanized anti-HER2 antibody *via* a cleavable dipeptide (valine-citrulline) linker. The humanized anti-HER2 antibody showed a higher affinity to HER2 (K_D , 5.0E-10M) compared with the approved HER2 therapeutic antibody trastuzumab (K_D , 1.9E-09M). The objective of the present study was to evaluate the selective targeted delivery of RC48-ADC through *in vitro* and *in vivo* experiments, including serum stability (using MMAE as a sensitive indicator), anti-tumour activity on a HER2-overexpressed cell line, subcellular distribution of antibodies and MMAE, and drug distribution in tumour-bearing mice. Our results showed that RC48-ADC was stable in the serum of humans and non-human primates. RC48-ADC exhibited higher anti-tumour potency on HER2-overexpressed SK-BR-3 compared with the naked antibody. The MMAE payload can be efficiently released in lysosomes after HER2-mediated endocytosis. In the tumour-bearing nude mice model, RC48-ADC administration achieved 200-fold higher MMAE exposure in the tumour than in the serum. We demonstrated the targeted delivery and release properties of RC48-ADC, which showed great promise for further clinical development in the treatment of HER2 overexpression in solid tumours.

Materials and Methods

Drug and Reagents

RC48 naked antibody and RC48-ADC were supplied by RemeGen, Ltd. (Yantai, Shandong, China). Trypsin, LysoTracker™ Green DND-26, and Vybrant™ DiO Cell-Labeling Solution

were obtained from Thermo Fisher Scientific (Waltham, MA, USA). pHAb Amine and Thiol Reactive Dye were purchased from Promega (Madison, WI, USA).

Tumour Cell Lines

The human breast carcinoma cell lines SK-BR-3 and MCF-7 were obtained from the American Type Culture Collection (ATCC; Manassas, VA, USA). They were maintained in high-glucose Dulbecco's Modified Eagle's Medium (DMEM) or Roswell Park Memorial Institute-1640 (RPMI-1640) supplemented with 10% foetal bovine serum (FBS; Hyclone, South Logan, UT, USA) until ready for use.

Xenograft Tumour Model

A Matrigel suspension of 1×10^7 NCI-N87 cells was subcutaneously (s.c.) injected into female nude BALB/cA mice. The mice were purchased from the Institute of Laboratory Animal Science, Chinese Academy of Medical Science (Shanghai, China) and housed in specific pathogen-free conditions. The mice were acclimatized to the new environment for 1 week before tumour inoculation and were allowed free access to food and water throughout the experiment. This study was approved by the Animal Ethics Committee of the Animal Center of National Center for Protein Sciences (Beijing).

Cell Proliferation Assay

MCF-7 and SK-BR-3 cells were incubated at densities of 2×10^3 and 5×10^3 cells per well, respectively, in 96-well E-plates. The cells adhered overnight and were then exposed to serial dilutions of RC48-ADC or naked antibody for 72 h. The drug concentrations were 0, 0.1, 0.5, 1, 2, and 5 $\mu\text{g}/\text{mL}$ for SK-BR-3 cells and 0, 0.1, 1, 10, 50, and 100 $\mu\text{g}/\text{mL}$ for MCF-7 cells. Cell indices were collected at intervals of 15 min.

Antibody Subcellular Distribution Assay

MCF-7 and SK-BR-3 cells were seeded in 35-mm confocal dishes with 1×10^5 cells in 1 mL of medium. The cells were pre-incubated with fluorescent antibody and fluorescent RC48-ADC at 0.1 $\mu\text{g}/\text{mL}$ in the dark for 6 h. After that, the medium was discarded, and cells were washed three times with phosphate-buffered saline (PBS); then, the cells were stained with MitoTracker™ Green FM or LysoTracker Green DND-26. Stained cells were rinsed with PBS three times and fixed in 4% paraformaldehyde. Finally, stained cells were

rinsed and visualized with laser scanning confocal microscopy (Olympus FV 1000-IX81, Tokyo, Japan) in the fluorescein isothiocyanate (FITC) and propidium iodide (PI) fluorescence channels. For the FITC channel, a laser at 488 nm was used for excitation, and emission was recorded from 500 to 530 nm; for the PI channel, a laser at 559 nm was used for excitation, and emission was recorded from 600 to 630 nm¹²⁻¹⁴.

MMAE Cellular Disposition

SK-BR-3 and MCF-7 cells were cultured in 6-well plates at 5×10^5 /well for 24 h, then, treated with 10 $\mu\text{g}/\text{mL}$ of RC48-ADC and 170 ng/mL of MMAE for 3, 6, and 24 h. At each time point, 100 μL of cell supernatant was collected for analysis. Cells were washed three times with PBS, and then, digested with trypsin. Lysis was performed by adding two volumes of ice-cold methanol, followed by a freeze-thaw cycle of 45 min at -20°C . Lysates were cleared by centrifugation at $10,000 \times g$ for 10 min at 4°C . They were then evaporated under nitrogen gas and reconstituted in acetonitrile/water before injection into the LC-MS/MS system.

Endocytosis

Cells were seeded in 6-well plates at 1×10^5 per dish and separately pre-treated with inhibitors, namely, amiloride hydrochloride (0.4 mg/L), chlorpromazine hydrochloride (CPZ, 0.4 mg/L), and cytosine (40 mg/L) for 20 h to inhibit endocytic pathways. Cells were rinsed three times with PBS after removing inhibitor solutions, and then, separately treated with fluorescent RC48 or fluorescent antibody alone at 0.1 $\mu\text{g}/\text{mL}$ for 6 h. Finally, after rinsing with PBS, the cells were stained with DiO and fixed in 4% paraformaldehyde, followed by visualization with laser scanning confocal microscopy in FITC and PI fluorescence channels sequentially.

In Vivo Drug Distribution

Forty-eight tumour-bearing mice were randomly divided into a blank control group, a low-dose group (1.5 mg/kg), and high-dose group (5 mg/kg). Three animals were used for each time point in each treatment group. Blood and tumour tissues were collected at 5 min, and 4, 24, 48, 72, 96, and 168 h after intravenous injection. Serum was collected from the blood samples. Tumour tissues were washed with normal saline and stored at -80°C prior to use. MMAE concentration in the serum and tumour was measured by LC-MS/MS.

Total and bound antibody concentration was measured by enzyme-linked immunosorbent assay (ELISA). Exposure of the circulatory system and tumours to MMAE was investigated, and the targeted transport and release of RC48-ADC were determined based on *in vivo* drug distribution.

Statistical Analysis

Statistical analysis was performed using Statistical Product and Service Solutions (SPSS) 22.0 software (IBM Corp., Armonk, NY, USA). Data were represented as mean \pm standard deviation (SD). The *t*-test was used for analysing measurement data. The differences between the two groups were analysed by using the Student's *t*-test. Comparison between multiple groups was done using One-way ANOVA test followed by post-hoc test (Least Significant Difference). $p < 0.05$ indicated significant difference.

Results

RC48-ADC Is Stable In Serum

The release rate of MMAE from ADC was selected as an assessment indicator. Human, rat, and mouse sera were used to prepare test samples at 50 $\mu\text{g}/\text{mL}$ and incubated at 4°C or 37°C . Samples were taken at 0, 4, and 24 h for quantitation of MMAE. In all three sera, MMAE was undetectable at 0 h. After incubation for 24 h at 37°C , 4.3% of MMAE in the mouse serum was released, but it was lower than 1% at other conditions. RC48-ADC was more stable at 4°C than at 37°C , more stable in human serum than in rat serum, and more stable in rat serum than in mouse serum. Thus, ADC generally was deemed to be very stable (Figure 1).

RC48-ADC Anti-Tumour Activity

We analysed the efficacy of RC48-ADC on two tumour cell lines with different levels of HER2 expression. Naked antibodies had no inhibitory effect on SK-BR-3 or MCF-7 cells. When RC48-ADC (at concentrations of 0.1 $\mu\text{g}/\text{mL}$ and above) was used to treat SK-BR-3 cells, cell resistance gradually decreased as the treatment time was prolonged (Figure 2). However, only ADC at a concentration of 10 $\mu\text{g}/\text{mL}$ and above had an inhibitory effect on the growth of MCF-7 cells. Naked antibodies showed no significant growth inhibition in either cell line. By contrast, RC48-ADC offered high-efficiency targeted inhibition of the growth and proliferation of both cell lines. In

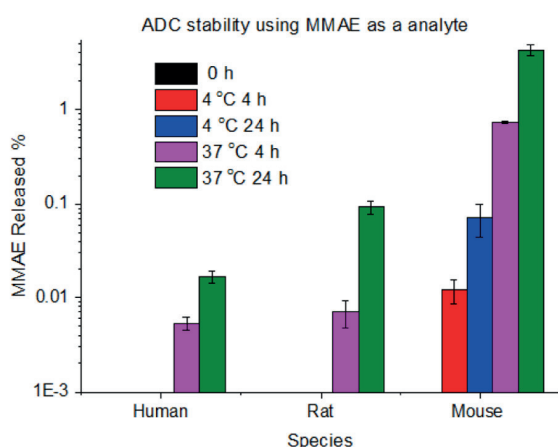


Figure 1. ADC stability using MMAE as an analyte.

summary, SK-BR-3 cells with upregulated HER2 expression were much more sensitive to ADC than MCF-7 cells with low HER2 expression.

Clathrin-Based and Caveolin-Based Endocytosis of RC48-ADC

To identify the proteins involved in the uptake pathways for naked antibody and RC48-ADC, pinocytosis, clathrin, and caveolae were inhibited with amiloride, CPZ, and cytosine, respectively^{12,13}. The safe concentration of CPZ, amiloride, and cytosine for SK-BR-3 and MCF-7 cells was 0.8, 1, and 50 mg/L, respectively (Figure 3A). Therefore, we used 0.4, 0.4, and 40 mg/L, respectively, of the compounds for inhibition. Confocal microscopy and Image J software were used to quantitate the uptake of DiO, fluorescent naked antibody, and fluorescent ADC (Figures 3B and 3C). With inhibition of pinocytosis by amiloride, cellular uptake of the naked antibodies and RC48-ADC decreased. With inhibition of clathrin and caveolae, cellular uptake of naked antibodies and RC48-ADC decreased significantly. The results showed that besides pinocytosis, clathrin-mediated and caveolin-mediated endocytosis were additional uptake pathways for naked antibodies and RC48-ADC.

RC48-ADC Trafficking to Lysosomes

Mitochondria and lysosomes were fluorescently labelled with MitoTracker™ Green FM and LysoTracker Green DND-26, respectively. SK-BR-3 cells were treated for 6 h with the fluorescence-labelled naked antibody and ADC (red) at 0.1 µg/mL. Then, the mitochondria

and lysosomes were stained (green). The distributions of the naked antibody and ADC highly overlapped with those of lysosomes, but much less colocalization was observed with mitochondria. Fluorescence co-localization indicated that naked antibodies were primarily transported to the lysosomes after cellular uptake, consistent with an earlier report¹⁵. However, after cellular uptake, RC48-ADC was still concentrated in the lysosomes (Figure 4A). Colocalization of RC48-ADC and organelles was quantitatively analysed using Image J software. The ratios of fluorescence intensity of RC48-ADC in organelles to total fluorescence intensity of the drug were analysed using the Manders overlap coefficient (MOC). As shown in Figure 4B, the MOCs of the naked antibody and RC48-ADC in the lysosomes were close to 1, but lower than 0.1 in the mitochondria. This demonstrated that the naked antibody and RC48-ADC were mainly distributed in the lysosomes. The fluorescence intensity of naked antibody and RC48-ADC in the lysosomes was also far higher than that in the mitochondria (Figure 4C), further confirming their concentration in lysosomes.

Intra- and Extracellular Distributions of MMAE

SK-BR-3 and MCF-7 cells were treated with 170 ng/mL MMAE or 10 µg/mL RC48-ADC for 3, 6, and 24 h. Therefore, the molar amount of MMAE and ADC administered was the same. Then, intracellular and culture MMAE concentrations were measured by an LC-MS/MS method. After treatment with MMAE, less than 6.5% of MMAE entered the cells, with intracellular uptake remaining unchanged for 24 h. After treatment with RC48-ADC, only a trace amount of free MMAE was detected in the culture medium of MCF-7 cells, with less than 100 pg/mL of free MMAE detected at 24 h (Figure 5). After treatment of SK-BR-3 cells with RC48-ADC, free MMAE was detected in both the cells and culture medium at multiple time points. MMAE concentration in the supernatant of SK-BR-3 cells increased as a function of treatment time. MMAE concentration in SK-BR-3 cells at 24 h was approximately 10 times that in MCF-7 cells. SK-BR-3 cells showed higher internalization of RC48-ADC and a higher released amount of MMAE. No significant differences were observed in MMAE concentrations inside and outside the cells of either line after direct administration of MMAE.

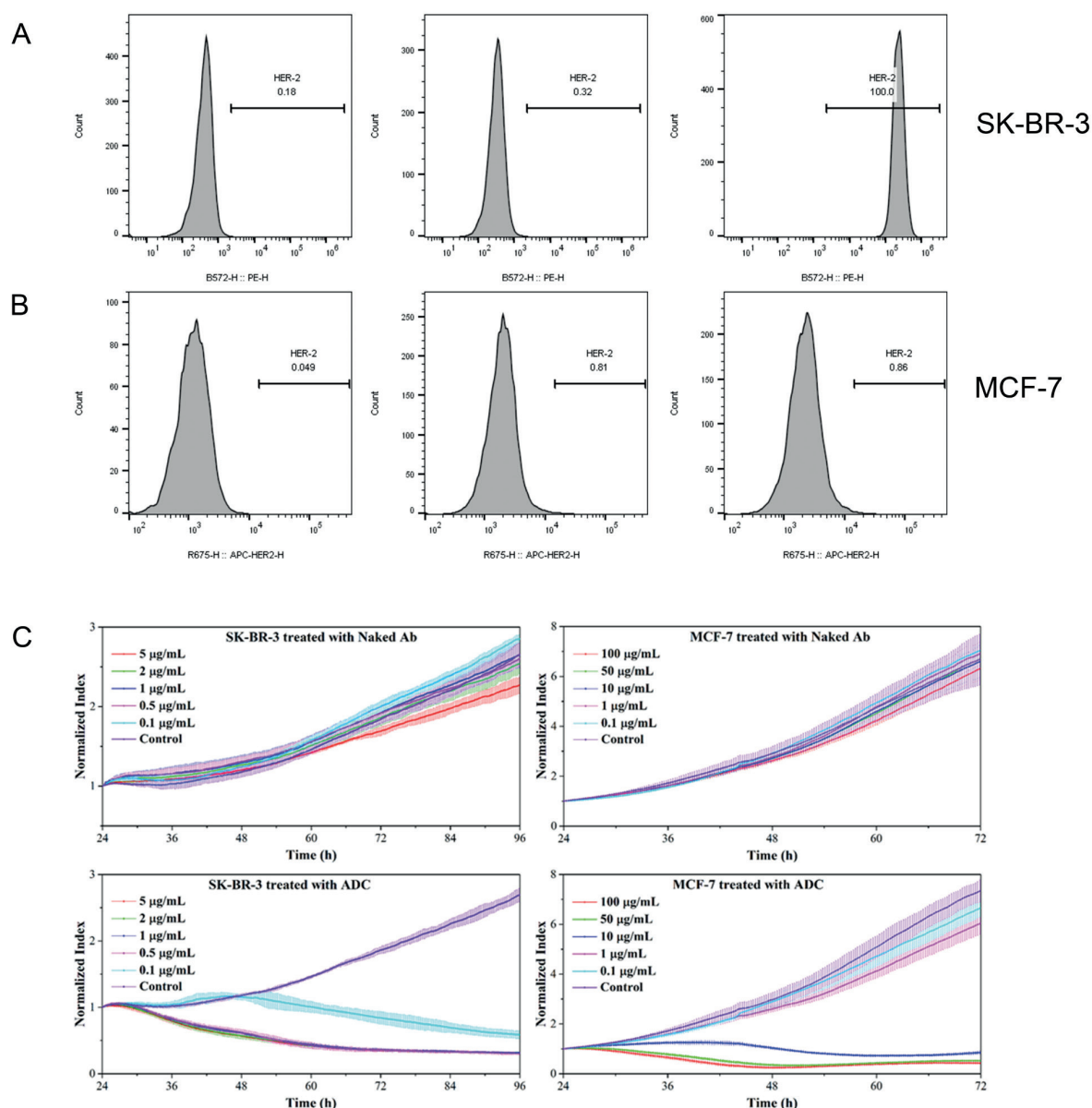


Figure 2. Inhibition of tumour-cell growth by RC48-ADC or antibody alone. **A**, HER2 expression in breast cancer cell lines SK-BR-3 and MCF-7 detected by flow cytometry. **(B)** SK-BR-3 and **(C)** MCF-7 tumour cell growth after treatment with RC48-ADC (left) and naked antibody (right).

MMAE is Targeted to Tumours after a Single Dose of RC48-ADC in Vivo

Female BALB/c nude mice were administered 1.5 mg/kg and 5 mg/kg of RC48-ADC by intravenous injection. The concentration-time profiles of MMAE and total antibodies in the serum samples and tumour tissues are plotted in Figure 6A and 6B. The pharmacokinetic parameters are shown in Table I. Serum concentration of RC48-ADC gradually decreased with time, whereas RC48-ADC

concentration in the tumour tissues remained more stable. The difference was that in the same dose group, peak concentrations of MMAE in tumour tissues and tumour exposure to MMAE were higher than those in serum. For the low-dose group, the C_{max} and exposure of MMAE in the tumour tissues were 33- and 260-fold higher than that in the serum, respectively; in the high-dose group, they were higher by 16- and 187-fold, respectively. These data suggested that MMAE was

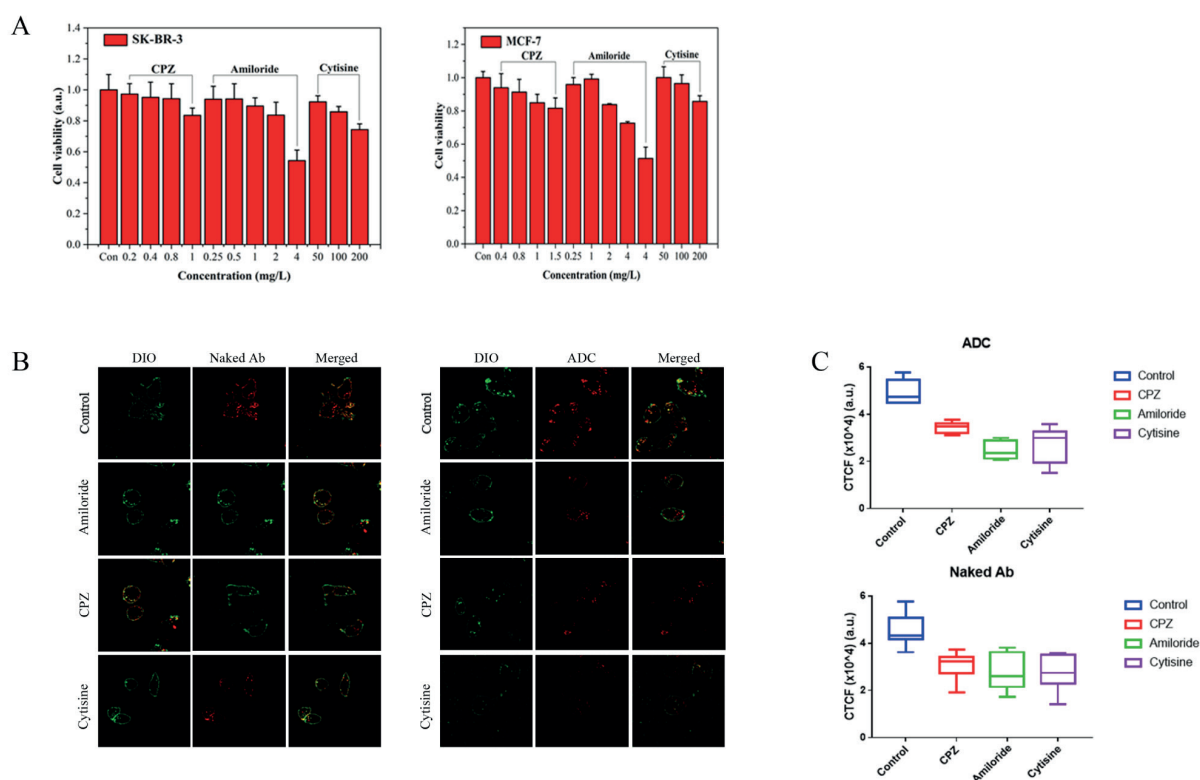


Figure 3. Cellular uptake of naked antibodies and RC48-ADC. **A**, For SK-BR-3 and MCF-7 cells, the safe concentrations of CPZ, amiloride, and cytisine were 0.8, 1, and 50 mg/L, respectively. **B**, and **C**, After different intracellular uptake pathways were inhibited, fluorescence intensities of the drugs were observed by fluorescence confocal microscopy, (magnification: 400 \times).

Table I. Antibodies and MMAE in serum and tumour tissues after administration of ADC to nude mice.

PK parameter	Unit	Serum			Tumour	
		total Ab	MMAE	ADC	total Ab	MMAE
Dose	(mg/kg)	1.5				
Tmax	hr	0.083	0.083	0.083	24	24
Cmax	ng/mL or ng/g	11494	1.73	11521	29.7	57.4
AUC _{0-t}	hr·ng/mL or hr·ng/g	365493	18.2	351458	1793.4	4746.5
Dose	(mg/kg)	5				
Tmax	hr	0.083	0.083	0.083	72	48
Cmax	ng/mL or ng/g	40863	7.86	40886	24.4	127
AUC _{0-t}	hr·ng/mL or hr·ng/g	1592005	72.4	1333100	2448	13531

better released in the tumour tissues and showed targeted cytotoxicity. As shown by area under the curve (AUC), the total antibody distribution in the tumour was less than 0.5% for both doses. Moreover, the distribution amount at the high dose was lower than that at the low dose, which was presumably related to target saturation.

Discussion

We found that relative to the effective concentration of the naked antibody, that of RC48-ADC for SK-BR-3 cells was approximately 50-fold lower. In other words, RC48-ADC is extremely cytotoxic at very low concentrations, which was its

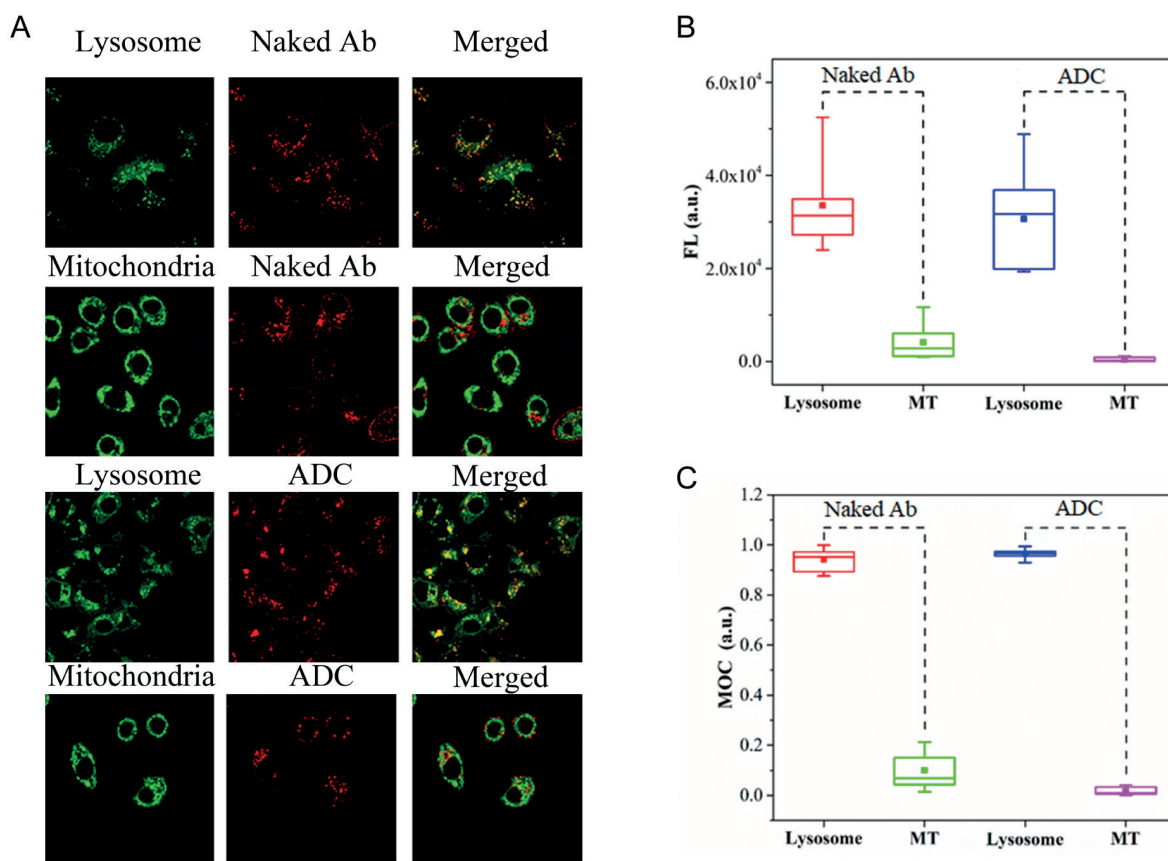


Figure 4. Distributions of naked antibodies and RC48-ADC in the lysosomes and mitochondria. **A**, SK-BR-3 cells treated with fluorescence-labelled naked antibody and ADC, (magnification: 400×). **B**, Ratios of fluorescence intensities of drug in organelles to total fluorescence intensities of drug. **C**, Products of the total fluorescence intensities of the drug; MOC represents the fluorescence intensity of the drug in organelles.

major advantage. In addition, the ADC was even more effective against the growth of SK-BR-3 cells, indicating better medicinal properties of RC48-ADC and reduction in off-target toxicity. We also compared the intracellular distributions of RC48-ADC and naked antibody, finding both primarily in lysosomes. It has been suggested that conjugation of the naked antibody to MMAE did not change its normal intracellular distribution. Massive concentration of RC48-ADC in lysosomes promoted the further release of MMAE. MMAE from SK-BR-3 cells (with high HER2 expression) also increased over time. This indicated that MMAE may be released from lysosomes and excreted by cells, which is known as the bystander effect, which can enhance efficacy on solid tumours^{2,16}. The most common way for drugs to enter cells is by pinocytosis. Our study shows that the amount of ADC entering the cells was decreased by inhibiting pinocytosis. With inhibition of clathrin and caveolae, intracellular

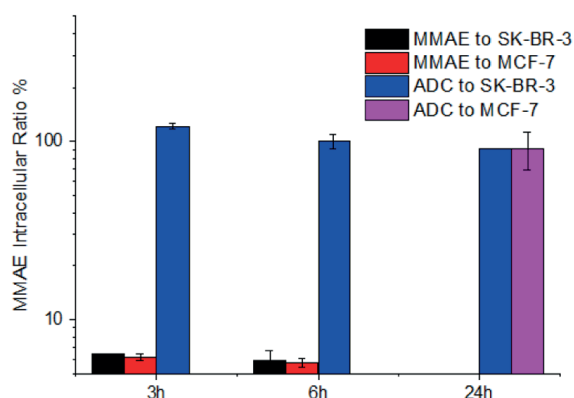


Figure 5. Intracellular and extracellular distributions of MMAE. SK-BR-3 and MCF-7 cells were treated with 170 ng/mL MMAE and 10 µg/mL RC48-ADC, respectively, for 3, 6, and 24 h.

uptake of RC48-ADC decreased significantly. Clathrin may be involved in the intracellular uptake of RC48-ADC, as it has been observed for

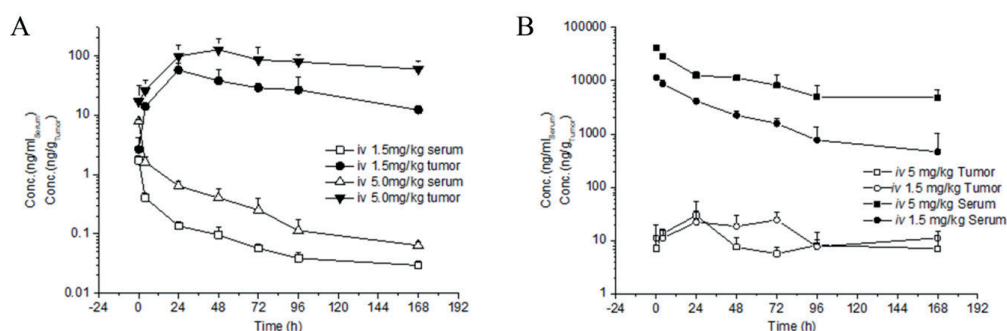


Figure 6. Concentration-time curves of MMAE and total antibodies in serum and tumour tissue. **A**, Concentrations of MMAE in tumour tissues and serum. **B**, Concentrations of total antibody in tumour tissues and serum.

the uptake of trastuzumab⁸. Our study indicated that intracellular uptake of RC48-ADC was also achieved through clathrin-mediated and caveolin-mediated endocytosis in addition to pinocytosis. To further verify the efficacy of RC48-ADC on the cellular level, the distributions of naked antibody and MMAE in serum and tumour tissues were determined in tumour-bearing mice. We found that the amount of RC48-ADC delivered to the target site accounted for less than 0.5% of the serum exposure to antibodies. Even at this proportion, MMAE was concentrated in tumour tissues, perhaps because after reaching the target site, RC48-ADC was degraded into toxin, which was then released. As more antibodies entered the target site and MMAE continued to be released, MMAE accumulated in the tumour tissues, thereby resulting in high, tumour-specific cytotoxicity. The PK parameters of the antibody were typical after iv infusion administration. The difference between the MMAE serum AUC and tumour AUC after the administration of the drug in the form of ADC showed that the serum exposure of MMAE can be reduced while greatly increasing tumour exposure, thus achieving the design concept of high efficiency and low systemic toxicity.

Conclusions

In summary, using MMAE as the stability indicator, the stability of the novel ADC can be assessed more sensitively and accurately. The targeting delivery and cytotoxic efficacy of RC48-ADC were assessed in cultured tumour cell lines and in a nude mouse model. The PK result of MMAE showed that RC48-ADC had a high efficiency for tumours and a low systemic toxicity, which was important to evaluate the advantage

of the novel ADC. A combination of laser confocal and LC-MS/MS methods were used to determine the distribution of antibodies and MMAE inside and outside the cell to intuitively illustrate the characteristics of ADC targeted transport and release. The intracellular targeting mechanism of the novel ADC was characterized. Our data suggest that the efficacy of RC48-ADC is better than that previously reported³. Our findings provide fundamental support for the clinical application of RC48-ADC.

Declaration of Funding Interests

This work was supported by Development Center for Medical Science & Technology National Health Commission of the People's Republic of China under Grant 2020ZX09201026.

Conflict of Interest

The Authors declare that they have no conflict of interests.

References

- 1) VERMA S, MILES D, GIANNI L, KROP IE, WELS LAU M, BASELGA J, PEGRAM M, OH DY, DIERAS V, GUARDINO E, FANG L, LU MW, OLSEN S, BLACKWELL K. Trastuzumab emtansine for HER2-positive advanced breast cancer. *N Engl J Med* 2012; 367: 1783-1791.
- 2) AMANI N, DORKOOSH FA, MOBEDI H. ADCs, as novel revolutionary weapons for providing a step forward in targeted therapy of malignancies. *Curr Drug Deliv* 2020; 17: 23-51.
- 3) WALKO CM, WEST HJ. Antibody drug conjugates for cancer treatment. *JAMA Oncol* 2019;5: 1648.
- 4) LAMBERT JM, BERKENBLIT A. Antibody-drug conjugates for cancer treatment. *Annu Rev Med* 2018; 69: 191-207.

- 5) KOVTUN YV, AUDETTE CA, YE Y, XIE H, RUBERTI MF, PHINNEY SJ, LEECE BA, CHITTENDEN T, BLATTLER WA, GOLDMACHER VS. Antibody-drug conjugates designed to eradicate tumors with homogeneous and heterogeneous expression of the target antigen. *Cancer Res* 2006; 66: 3214-3221.
- 6) CHORITZ H, BUSCHE G, KREIPE H. Quality assessment of HER2 testing by monitoring of positivity rates. *Virchows Arch* 2011; 459: 283-289.
- 7) MITRASINOVIC PM. Epidermal growth factor receptors: a functional perspective. *Curr Radiopharm* 2012; 5: 29-33.
- 8) BUCKEL L, SAVARIAR EN, CRISP JL, JONES KA, HICKS AM, SCANDERBEG DJ, NGUYEN QT, SICKLICK JK, LOWY AM, TSIEN RY, ADVANI SJ. Tumor radiosensitization by monomethyl auristatin E: mechanism of action and targeted delivery. *Cancer Res* 2015; 75: 1376-1387.
- 9) LI H, YU C, JIANG J, HUANG C, YAO X, XU Q, YU F, LOU L, FANG J. An anti-HER2 antibody conjugated with monomethyl auristatin E is highly effective in HER2-positive human gastric cancer. *Cancer Biol Ther* 2016; 17: 346-354.
- 10) YAO X, JIANG J, WANG X, HUANG C, LI D, XIE K, XU Q, LI H, LI Z, LOU L, FANG J. A novel humanized anti-HER2 antibody conjugated with MMAE exerts potent anti-tumor activity. *Breast Cancer Res Treat* 2015; 153: 123-133.
- 11) BARGH JD, ISIDRO-LLOBET A, PARKER JS, SPRING DR. Cleavable linkers in antibody-drug conjugates. *Chem Soc Rev* 2019; 48: 4361-4374.
- 12) LI Q, ZHOU T, WU F, LI N, WANG R, ZHAO Q, MA YM, ZHANG JQ, MA BL. Subcellular drug distribution: mechanisms and roles in drug efficacy, toxicity, resistance, and targeted delivery. *Drug Metab Rev* 2018; 50: 430-447.
- 13) JIANG L, LI X, LIU L, ZHANG Q. Cellular uptake mechanism and intracellular fate of hydrophobically modified pullulan nanoparticles. *Int J Nanomedicine* 2013; 8: 1825-1834.
- 14) PLUMMER EM, MANCHESTER M. Endocytic uptake pathways utilized by CPMV nanoparticles. *Mol Pharm* 2013; 10: 26-32.
- 15) SHARMA A, VAGHASIYA K, RAY E, VERMA RK. Lysosomal targeting strategies for design and delivery of bioactive for therapeutic interventions. *J Drug Target* 2018; 26: 208-221.
- 16) MOODY PR, SAYERS EJ, MAGNUSSON JP, ALEXANDER C, BORRI P, WATSON P, JONES AT. Receptor crosslinking: a general method to trigger internalization and lysosomal targeting of therapeutic receptor:ligand complexes. *Mol Ther* 2015; 23: 1888-1898.